PHYSICAL REVIEW A **84**, 021803(R) (2011)

Optical eigenmode imaging

Anna Chiara De Luca, Sebastian Kosmeier, Kishan Dholakia, and Michael Mazilu*
SUPA-School of Physics and Astronomy, University of St Andrews, North Haugh, KY16 9SS, St Andrews, UK
(Received 2 March 2011; published 15 August 2011)

We present an indirect imaging method that measures both amplitude and phase information from a transmissive target. Our method is based on an optical eigenmode decomposition of the light intensity and the first-order cross correlation between a target field and these eigenmodes. We demonstrate that such optical eigenmode imaging does not need any *a priori* knowledge of the imaging system and corresponds to a compressive full-field sampling, leading to high image extraction efficiencies. Finally, we discuss the implications with respect to second-order correlation imaging.

DOI: 10.1103/PhysRevA.84.021803 PACS number(s): 42.30.−d, 42.40.−i

The last two decades have seen the emergence of interest in schemes for interaction-free imaging [1] and indirect imaging [2] in both the quantum and classical domain [3]. Such schemes inherently use light fields to image that have themselves never scattered from the object. Prominent among these schemes has been the concept of ghost imaging [4–7]. These methods allow the image of an unknown object to be nonlocally reconstructed by the intensity correlation measurements between two light fields. The light that illuminates the object is typically collected by a single-pixel detector that itself has no spatial resolution. The underlying physics of ghost imaging has seen major debate about its classical and quantum implications, as both entangled source and thermal light can be used. While a powerful concept, ghost imaging does not inherently reveal phase information about an object, as it relies on a second-order correlation for its implementation [2,8]. Additionally, the resolution of the recovered images is determined by the size of the speckle placed on the object plane [4]. Any imperfections or aberrations within the system may not be readily dealt with in such a system. A significant step forward would be an indirect imaging scheme based on correlation measurements that could retrieve both amplitude and phase and inherently accommodate issues relating to aberrations or imperfections within the optical system.

In this Rapid Communication, we realize such a scheme using the concept of optical eigenmodes [9,10]. We split the laser light into two different beams. One beam does not interact with the target, but illuminates a high-resolution CCD camera (multipixel detector). The other one interrogates, in transmission, the target (or sample) and then illuminates a photodiode (single-pixel detector) providing no spatial resolution. The transmission wave front of this beam is decomposed, using an optical lock-in amplification technique, onto an orthogonal set of optical eigenmodes. The lock-in amplification corresponds to performing a first-order cross correlation and as such is distinct from present ghost-imaging techniques. In turn, this leads to the retention of the phase information of the object. Further, our approach foregoes point-by-point scanning and allows rapid full-field image extraction [11].

The outline of this Rapid Communication is as follows. First the concept of the optical eigenmodes is briefly reviewed, and then we discuss the problem of combining eigenmodes and indirect imaging. We introduce the experiment and show an application of the eigenmode method for indirect imaging of a target. We demonstrate the advantage of optical eigenmode imaging in terms of resolution and phase information. Finally, we show the relationship between optical eigenmodes and the second-order correlation function.

Method. To define the intensity optical eigenmodes [10], we decompose a linearly polarized electromagnetic field E into a superposition of N monochromatic ($e^{i\omega t}$) "test" fields:

$$E = \sum_{j=1}^{N} a_j^* E_j; \quad E^* = \sum_{k=1}^{N} E_k^* a_k. \tag{1}$$

Here we consider the field intensity $m^{(I)}$ integrated over a region of interest (ROI), as defined by

$$m^{(I)}(E) = \int_{\mathrm{ROI}} d\sigma\, E \times E^*, \tag{2}$$

which is valid for linearly polarized light and not tightly focused beams. The ROI represents the detector active area. Equation (2) can be written in a general quadratic matrix form, $m^{(I)}(E) = \sum_{j,k} a_j^* M_{jk} a_k = \mathbf{a}^* \mathbf{M} \mathbf{a}$, where the elements M_{jk} are constructed by combining the fields E_j and E_k for $j,k = 1,\ldots,N$ as $M_{jk} = \int_{\mathrm{ROI}} d\sigma\, E_j \times E_k^*$. The optical eigenmodes are defined by

$$\mathbb{E}_\ell = \frac{1}{\sqrt{\lambda^\ell}} \sum_{j=1}^{N} v_{\ell j}^* E_j; \quad \mathbb{E}_\ell^* = \frac{1}{\sqrt{\lambda^\ell}} \sum_{j=1}^{N} v_{\ell j} E_j^*, \tag{3}$$

with $\sum_j M_{jk} v_{\ell j} = \lambda^\ell v_{\ell k}$, where λ^ℓ is an eigenvalue and $v_{\ell j}$ is the associated eigenvector. The matrix M_{jk} shows two important properties. First, it is Hermitian, meaning that all the eigenvalues (λ^ℓ) are real and can be ordered, where $\lambda^{\ell=1}$ is the largest eigenvalue, $\lambda^{\ell=2}$ is the second largest eigenvalue, and so on. Second, two eigenvectors corresponding to different eigenvalues are orthogonal, which means that $\int_{\mathrm{ROI}} d\sigma\, \mathbb{E}_j \times \mathbb{E}_k^* = \delta_{jk}$. As a matter of fact, each of these eigenvectors $v_{\ell j}$ corresponds to a superposition of the initially considered fields. An unknown field T can be decomposed onto the eigenmodes using its projection defined by $c_\ell^* = \int_{\mathrm{ROI}} d\sigma\, T \times \mathbb{E}_\ell^*$, where c_ℓ corresponds to the complex decomposition coefficients of the field T in base $\mathbb{E}_\ell$. If the $\mathbb{E}_\ell$ fields form a complete base, we can perfectly reconstruct the unknown field T from the projection using $T = c_\ell^* \mathbb{E}_\ell$. We

*michael.mazilu@st-andrews.ac.uk

remark that the completeness of the base is dependent on the initial fields probing all the degrees of freedom available.

Optical eigenmode imaging is based upon a direct measure of the projection coefficients c_ℓ^* and the experimental reconstruction of the unknown field T, that is essentially the transmission function through the target.

Experiment. The basic setup used for the optical eigenmode imaging is shown in Fig. 1. A He-Ne laser beam (Thorlabs, $\lambda = 633$ nm, $P_{\max} = 10$ mW) is expanded to fill the aperture of a spatial light modulator (SLM) (Hamamatsu LCOS-SLM X10468, the resolution is 600×800 pixels, the pixel size is 20×20 μm^2, the refresh rate is 60 Hz), and then phase modulated in the first-order configuration [12]. This configuration allows us to achieve both phase and intensity modulation. The beam is divided into two symmetric parts by a 50:50 beam splitter. The reflected beam interrogates a transmissive target placed in the focal plane of the Fourier lens (L3 = 75 cm). A second Fourier lens (L4 = 10 cm) integrates the transmitted light on a photodiode providing no spatial resolution. The transmitted beam is focused directly on a high-resolution CCD camera (Basler pilot piA 640–210 mg, resolution is 648×488 pixels, pixel size is 7.4×7.4 μm^2) without interacting with the target. By projecting the optical eigenmodes on the target, it is possible to reproduce the target image on the CCD camera.

The experiment consists of two steps. First, it is necessary to determine the optical eigenmodes ($\mathbb{E}_\ell$) in the CCD camera plane by interfering the test fields E_j created in the SLM plane. Next, we select the n most intense optical eigenmodes and interfere them with a reference signal (E_{ref}). The reference signal (E_{ref}) is randomly phase encoded [13] on the same SLM and thus shares the same optical path as the test field. In this way, we can reconstruct the relative amplitude and phase of the linearly polarized fields F_j on the CCD camera:

$$F_j = \frac{1}{R}\sum_{p=0}^{R-1} e^{i2\pi p/R}|E_{\text{ref}} + e^{-i2\pi p/R}E_j|^2, \tag{4}$$

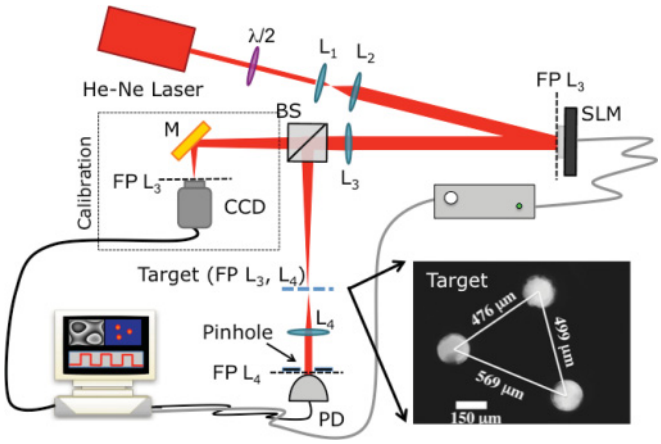

FIG. 1. (Color online) The experimental setup used to perform indirect imaging with the optical eigenmode formalism. The inset shows a scheme of the target of three holes used in our experiment. Abbreviations: L, lens; M, mirror; BS, beam splitter; FP, focal plane; PD, photodiode.

where R is an integer number greater than 3. This procedure can be seen as a phase-sensitive lock-in technique where the reference beam E_{ref} corresponds to a reference signal with respect to which the phase and amplitude of E_j is measured. This is performed by measuring R times the intensity on the CCD camera while changing the relative phase between the reference and the test field. These intensities are then combined in Eq. (4) in an inverse Fourier transform, delivering a measure proportional to the complex test field E_j. This approach generalizes the method presented in [10]. We remark here that due to the lock-in technique, using a larger number of measures R experimentally delivers a better signal-to-noise ratio. Here, we used $R = 4$. The intensity operator M_{jk} is given by

$$M_{jk} = \int_{\text{ROI}} d\sigma \mathrm{F}_j \times \mathrm{F}_k^*, \tag{5}$$

where ROI is a region of interest on the CCD camera.

In the second experimental step, we project the optical eigenmode on the target (T) using a first-order cross correlation with the reference beam. The projection coefficients c_k are related to the signal s_k measured by the single-pixel detector (PD) as follows:

$$\begin{aligned} s_k &= \frac{1}{R}\sum_{p=0}^{R-1} e^{i2\pi p/R}\left|\int_{\text{ROI}} d\sigma T \times (E_{\text{ref}} + e^{-i2\pi p/R}\mathbb{E}_k)\right|^2 \\ &= \int_{\text{ROI}} d\sigma T \times E_{\text{ref}}^* \times \int_{\text{ROI}} d\sigma T^* \times \mathbb{E}_k \\ &= c_k \int_{\text{ROI}} d\sigma T \times E_{\text{ref}}^*, \end{aligned} \tag{6}$$

where $\int_{\text{ROI}} d\sigma T \times E_{\text{ref}}^*$ gives the coupling coefficient to the target and is essentially a constant value. Therefore, from the signal acquired on the PD, we can measure the coefficients c_k, which makes it possible to reconstruct the complex target field. Finally, using a Dirac distribution target field, we can

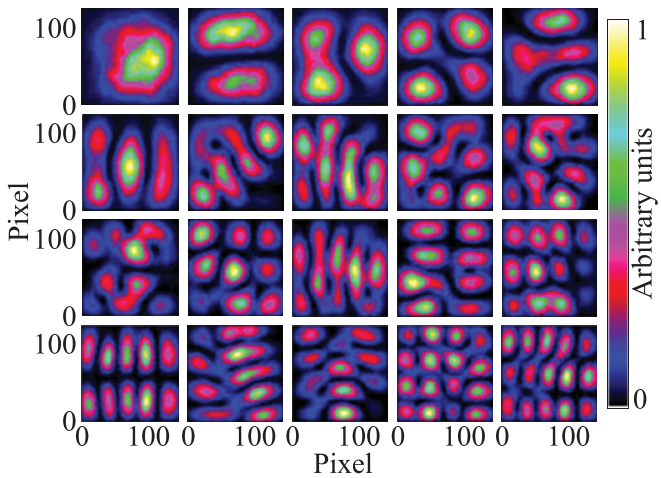

FIG. 2. (Color online) Examples of the principal experimental intensity optical eigenmodes. The resolution of each image is 120×120 pixels.

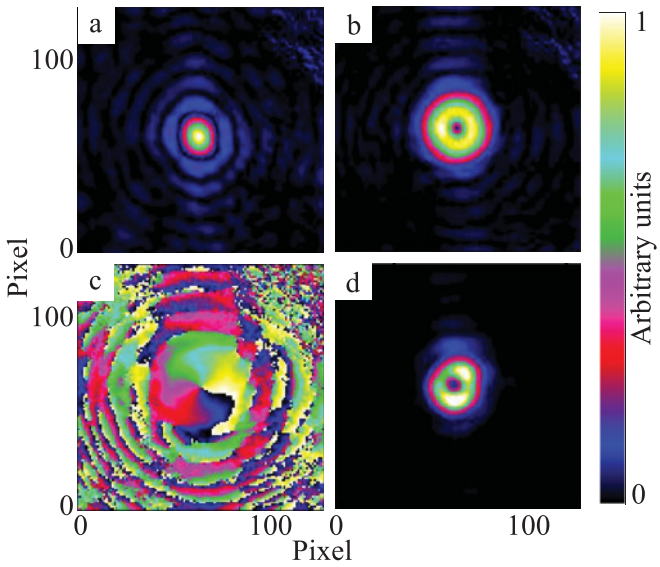

FIG. 3. (Color online) Experimental optical eigenmode imaging of a Laguerre-Gauss (LG) beam. (a) Point-spread function (PSF) obtained by combining 147 intensity optical eigenmodes. (b) Theoretical intensity and (c) phase of a decomposed LG beam [intensity scale bar is from 0 (black) to 2π (white)]. (d) Experimental reconstruction of the LG beam using the 147 optical eigenmodes.

deduce the point-spread function E_{PSF}, which determines the resolution of the optical eigenmode imaging method,

$$E_{\mathrm{PSF}} = \sum_{j=1}^{N} \mathbb{E}_j \int_{\mathrm{ROI}} \delta(r - r_0)\mathbb{E}_j^* d\sigma. \tag{7}$$

Results and discussion. In our experiment, we used $N = 1353$ masks consisting of 33 horizontal and 41 vertical independent deflection angles to determine the intensity optical eigenmodes ($\mathbb{E}_\ell$) in the CCD camera plane. After the Fourier lens (L3), these deflections correspond to a regular grid scan over an area of 1.2 by 1.3 mm. The reference field (E_{ref}) was chosen to be the median beam out of the 1353 beams used. The first 20 experimental intensity optical eigenmodes are shown in Fig. 2, displaying visually an orthogonal behavior similar to TEM modes.

From the experimental intensity optical eigenmodes, we select the ones with an efficiency above 0.1% with respect to the maximum possible, giving us typically around 140 eigenmodes. This corresponds to a tenfold image data reduction when compared to the initial number of test fields ($N = 1353$). Further, we noticed no clear increase in the number of suitable eigenmodes when increasing N. The quality of this optical compression technique can be assessed experimentally by determining the point-spread function (PSF) (7), showing the loss of image information when reconstructing a Dirac distribution field. Figure 3(a) shows the experimental PSF obtained by combining $N = 147$ intensity optical eigenmodes representing the resolution limit of the system. Further, we numerically project the experimental eigenmode fields onto a simulated Laguerre-Gaussian target with a unit vortex charge. The theoretical reconstructed field is displayed in Figs. 3(b) and 3(c) as field intensity and phase, respectively. Figure 3(d) shows the intensity on the CCD camera when the SLM displays the optical eigenmode superposition corresponding to $T = \sum_\ell c_\ell^* \mathbb{E}_\ell$. These figures show that optical eigenmode imaging provides both phase and intensity information.

For the indirect imaging, we used a target consisting of three holes each with a diameter of $\sim$150 μm (see Fig. 1 for more details). Figure 4(a) shows the conventional transmission image of the target obtained by scanning the laser spot, using the initial 1353 deflection masks, through the holes. In this figure, we plot the signal intensity detected by the single-pixel detector (PD) for each angle of the light scanning. By contrast, Figs. 4(b) and 4(c) show the indirect image obtained, respectively, through numerical and experimental optical eigenmode superpositions, on the CCD camera. A direct comparison of the theoretical superposition [Fig. 4(b)] and the experimental one [Fig. 4(c)] clearly reveals a good agreement. These results suggest that the numerical and the experimental distributions verify $s_k \propto c_k$, demonstrating the linearity of our optical system. Further, by comparing Figs. 4(a) and 4(c), we can clearly observe an enhancement in the resolution of the optical eigenmode image with respect to the conventional transmission image using the initial scanning "test" fields.

Remarkably, the optical eigenmodes described above simplify the first-order correlation functions. Indeed, we

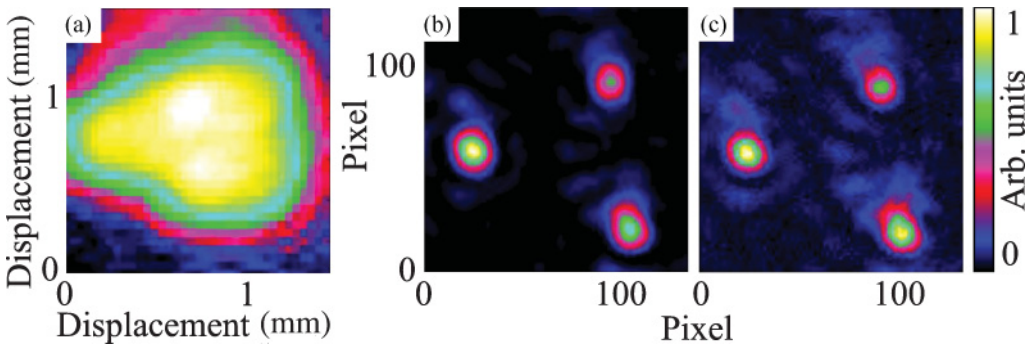

FIG. 4. (Color online) Indirect imaging of a target consisting of three holes. (a) Conventional transmission image of the target reconstructed from the intensity signal collected by the PD as a function of the beam displacement in the target plane. (b) Corresponding numerical indirect intensity image of the target. (c) Experimental indirect optical eigenmode image.

have

$$G^{(1)}(\tau) = \int_{\mathrm{ROI}} \langle E(t)E^*(t+\tau)\rangle d\sigma = e^{-i\omega\tau}\left\langle \sum_{j,k} a_j^* M_{jk} a_k \right\rangle = \sum_{j,k} G_{jk}^{(1)}(\tau), \qquad (8)$$

with $G_{jk}^{(1)}(\tau) = \int_{\mathrm{ROI}} \langle \mathbb{E}_j(t)\mathbb{E}_k^*(t+\tau)\rangle d\sigma = e^{-i\omega\tau}\delta_{jk}$, where the symbol $\cdots$ indicates the ensemble averaging. This relationship shows that the optical eigenmodes are independent with respect to the first-order correlation function, i.e., amplitude and phase fluctuations of two different eigenmodes are not correlated. This implies that any random thermal fluctuations of the illumination source can be decomposed into independent fluctuations, with each corresponding to an eigenmode. We also remark that the phase information is maintained in the first-order correlation process. It is these two properties that make optical eigenmode indirect imaging possible. Additionally, illuminating the target directly with the eigenmodes does not rely on random thermal fluctuations to explore their Hilbert space, but instead each independent optical degree of freedom of the illumination is used successively to build up the final image in an efficient way.

Another interesting aspect of the optical eigenmode decomposition of the illuminating light field is the behavior of the second-order correlation function between two different detectors (D_1 and D_2). This can be represented as $g^{(2)} = \langle(\mathbf{a}^*\mathbf{M}^{(1)}\mathbf{a})(\mathbf{a}^*\mathbf{M}^{(2)}\mathbf{a})\rangle$, where the measures $\mathbf{a}^*\mathbf{M}^{(1)}\mathbf{a}$ and $\mathbf{a}^*\mathbf{M}^{(2)}\mathbf{a}$ correspond to the intensity for each detector described using each one's matrix intensity operators $\mathbf{M}^{(1)}$ and $\mathbf{M}^{(2)}$. For each of these operators, we can define the null space as the superposition of eigenmodes having zero eigenvalue. Considering these null spaces, we can define four physically distinguishable cases: (1) the intersection subspace of the two null spaces corresponds to modes of light that do not interact with either of the two detectors, (2) the relative complement of $\mathbf{M}^{(1)}$ null space in $\mathbf{M}^{(2)}$ null space corresponds to optical fields that are detected by D_1 while not influencing the measure on detector D_2, (3) the same as the second case, with indices 1 and 2 exchanged, and (4) the complement to all previous cases defines a field subspace where the measure on one detector influences the measure on the other. In short, using this decomposition, it is possible to describe four distinct possible interactions: no field on either detector, field only on detector D_1, field only on detector D_2, and field on both detectors. Finally, the second-order correlation function $g^{(2)}$ is zero for any single superposition of optical eigenmodes taken from any single one of the first three cases, and nonzero for the fourth case. This means that the second-order correlation function of independent detectors (cases 2 and 3) is zero for a single (not ensemble averaged) intensity measurement.

In conclusion, we show that optical eigenmode imaging allows the indirect complex reconstruction of a transmissive target. This method is based on the decomposition of the field into intensity optical eigenmodes. The decomposition coefficients are directly measured by the first-order cross correlation between the unknown target field T and the optical eigenmodes. Superimposing the optical eigenmodes with the decomposition coefficients yields the reconstructed target field T. Importantly, the complex decomposition coefficients provide phase information, potentially allowing the reconstruction of optical-path length information of the target akin to transmission optical tomography. Further, we show that the optical eigenmode imaging corresponds to a compressive full-field sampling, improving the imaging speed without loss of details and enabling fast spectroscopic applications such as wide-field Raman imaging. Finally, we related the optical eigenmodes approach to the first-order and second-order correlation functions. In future work, we aim to explore the implications of optical eigenmodes in the field of quantum optics.

ACKNOWLEDGMENTS

We thank the UK Engineering and Physical Sciences Research Council for funding. The work was also partly funded by the CSO and CR-UK/EPSRC/MRC/DoH (England) Imaging Programme. A.C.D.L. received support from an EPSRC Fellowship and K.D. received support from a Royal Society-Wolfson Merit Award.

[1] A. G. White, J. R. Mitchell, O. Nairz, and P. G. Kwiat, Phys. Rev. A **58**, 605 (1998).
[2] R. S. Bennink, S. J. Bentley, and R. W. Boyd, Phys. Rev. Lett. **89**, 113601 (2002).
[3] B. I. Erkmen and J. H. Shapiro, Adv. Opt. Photon. **2**, 405 (2010).
[4] F. Ferri, D. Magatti, A. Gatti, M. Bache, E. Brambilla, and L. A. Lugiato, Phys. Rev. Lett. **94**, 183602 (2005).
[5] G. Scarcelli, V. Berardi, and Y. Shih, Phys. Rev. Lett. **96**, 063602 (2006).
[6] J. H. Shapiro, Phys. Rev. A **78**, 061802 (2008).
[7] Y. Bromberg, O. Katz, and Y. Silberberg, Phys. Rev. A **79**, 053840 (2009).
[8] W. Gong and S. Han, Phys. Rev. A **82**, 023828 (2010).
[9] M. Mazilu, J. Opt. A **11**, 094005 (2009).
[10] M. Mazilu, J. Baumgartl, S. Kosmeier, and K. Dholakia, Opt. Express **19**, 933 (2011).
[11] M. A. Herman and T. Strohmer, IEEE Trans. Signal Process. **57**, 2275 (2009).
[12] R. Di Leonardo, F. Ianni, and G. Ruocco, Opt. Express **15**, 1913 (2007).
[13] G. Spalding, J. Courtial, and R. D. Leonardo, in *Structured Light and its Applications: An Introduction to Phase-Structured Beams and Nanoscale Optical Forces*, edited by D. L. Andrews (Elsevier, Academic, 2008).